AIP | Journal of Applied Physics

The magnetocaloric effect of partially crystalline Fe-B-Cr-Gd alloys

J. Y. Law, V. Franco, and R. V. Ramanujan

Citation: Journal of Applied Physics **111**, 113919 (2012); doi: 10.1063/1.4723644
View online: http://dx.doi.org/10.1063/1.4723644
View Table of Contents: http://scitation.aip.org/content/aip/journal/jap/111/11?ver=pdfcov
Published by the AIP Publishing

The magnetocaloric effect of partially crystalline Fe-B-Cr-Gd alloys

J. Y. Law,[1,2] V. Franco,[2] and R. V. Ramanujan[1,a)]
[1]*School of Materials Science and Engineering, Nanyang Technological University, Singapore 639798*
[2]*Dpto. Física de la Materia Condensada, ICMSE-CSIC, Universidad de Sevilla, P.O. Box 1065, 41080 Sevilla, Spain*

(Received 8 December 2011; accepted 29 April 2012; published online 13 June 2012)

The influence of annealing temperature and crystallization on the magnetocaloric effect (MCE) of Fe-B-Cr-Gd partially crystalline alloys was studied. Although the alloys exhibited dissimilar devitrification behavior, all the alloys exhibited MCE behavior consistent with a phenomenological universal curve and theoretical power law expressions of the magnetic field dependence of MCE. The T_C of partially crystalline $Fe_{75}B_{12}Cr_8Gd_5$ alloys increased with increasing annealing temperatures. However, peak magnetic entropy change and refrigerant capacity values remained relatively constant, suggesting that these alloys are promising for active magnetic regenerator applications. © *2012 American Institute of Physics*. [http://dx.doi.org/10.1063/1.4723644]

I. INTRODUCTION

The magnetocaloric effect (MCE) is the induced temperature change of a magnetic material when it is adiabatically subjected to a varying magnetic field. This effect can be exploited in novel energy efficient and environmentally friendly magnetic cooling systems. Hence, this area of research has attracted intensive attention in the search for novel magnetocaloric materials (MCM).[1–4] The MCE generally peaks near the phase transition of a magnetic material, i.e., its Curie temperature (T_C). The search for new MCM for commercial applications has concentrated mainly on affordable MCM with tunable T_C and reasonable MCE. MCM studied so far are mainly Gd based alloys as well as "giant" MCE materials (e.g., $Gd_5Si_2Ge_2$) typically exhibiting first order magnetostructural phase transitions (FOPT). These materials are expensive and have high rare earth content. MCM with FOPT exhibit detrimental hysteresis losses which can lead to lower frequency response and will decrease the operating frequency in refrigerator applications. Iron-based amorphous alloys are a possible solution to such concerns since they offer affordable material and fabrication costs, reasonable MCE, low magnetic hysteresis, high electrical resistivity, and tunable T_C.[5–7]

The performance evaluation parameters of MCE include the peak magnetic entropy change ($|\Delta S_M^{pk}|$) and refrigerant capacity (RC). In addition to minimizing hysteresis losses, other research efforts include development of nanocrystalline alloys[8–10] and multilayered MCM.[11–13] Such multilayers of MCM exhibit much higher temperature span and RC due to the presence of multiple layers, each with own T_C and $|\Delta S_M^{pk}|$. In addition, the temperature span and RC can also be improved in an active magnetic regenerative cycle due to its distinctive feature of having every section of the MCM bed undergo its own unique local magnetic Brayton cycle.[14] In this case, the MCM functions as a refrigerant and also a thermal regenerator, enabling conventional regenerator properties be combined with the MCE.[15]

Fe-B-Cr-Gd amorphous alloys have been studied previously[16,17] and exhibit enhanced MCE properties compared to both $Fe_{80}B_{12}Cr_8$ alloys[18] as well as the well known giant MCE $Gd_5Si_2Ge_{1.9}Fe_{0.1}$ alloy.[19] The need to tailor the MCE of materials for active magnetic regenerative applications has become the focus of intense research, hence understanding the role of crystallization on the MCE of initially amorphous alloys is significant. $Fe_{79}B_{12}Cr_8Gd_1$ and $Fe_{75}B_{12}Cr_8Gd_5$ alloys were partially crystallized from their amorphous precursors, to study the effect of annealing on the MCE of Fe-B-Cr-Gd alloys. Although the alloys exihibit dissimilar devitrification behavior and samples present different crystalline volume fractions, it has been found that a phenomenological universal curve and theoretical power law expressions of magnetic field dependence of MCE are applicable to these partially crystalline alloys. The $|\Delta S_M^{pk}|$ of these alloys compare favorably with those of Mo-containing Finemet-type nanocrystalline MCM (Ref. 5) as well as several other Fe-based nanocrystalline MCM.[9,20–22]

II. EXPERIMENTAL

Melt-spun ribbons of nominal composition $Fe_{80-x}B_{12}Cr_8Gd_x$ (x = 1 and 5)[16] were annealed under protective argon atmosphere at temperatures ranging from 720 to 880 K. These alloy compositions are denoted as Gd1 and Gd5 alloys, respectively. The temperatures were selected, based on the differential scanning calorimetry (DSC) results (Fig. 1) of the melt-spun ribbons, so as to yield partially crystalline Gd1 and Gd5 alloys. To understand the crystallization behavior of these alloys, the ribbons were heated to the primary crystallization stage in three conditions: (1) annealed to the onset temperature, (2) intermediate stage of the process, and (3) heated to the peak temperature (Fig. 1). In all cases, the samples were heated and cooled at the rate of 10 and 20 K min^{-1}, respectively. The ribbons are denoted according to these three conditions: Gd1 partially crystalline alloys—Gd1 (720 K), Gd1 (730 K), Gd1 (740 K); Gd5

a)Author to whom correspondence should be addressed. Electronic mail: Ramanujan@ntu.edu.sg. Tel.: +65 67904342. Fax: +65 67909081.

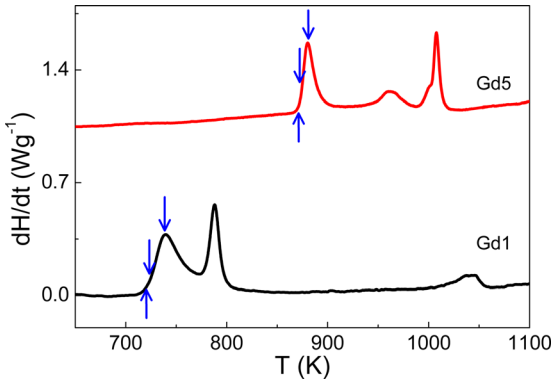

FIG. 1. DSC results of melt-spun Gd1 and Gd5 alloys.

partially crystalline ribbons—Gd5 (872 K), Gd5 (876 K), Gd5 (880 K).

The microstructure of the ribbons was characterized by x-ray diffraction (XRD) using a Bruker D8 Advance diffractometer and by transmission electron microscopy (TEM). The micrographs were collected digitally using a JEOL JEM 2100 ($C_S = 0.5$ mm) TEM operated at 200 kV. XRD measurements were performed using CuKα radiation ($\lambda = 0.154$ nm) in the scan range from 10° to –80° and scan speed of 0.02°/step. The composition was characterized by electron microprobe analysis (EPMA) using a JEOL JXA-8530 F operated at 15 keV. The field and temperature dependence of magnetization was measured by a Lakeshore 7407 vibrating sample magnetometer (VSM) for magnetic fields up to 15 kOe.

III. RESULTS AND DISCUSSION

The XRD patterns of the partially crystalline Gd1 and Gd5 alloys are shown in Fig. 2. Well-resolved peaks were observed for both alloys when the ribbons were annealed to temperatures in the range of 720–740 K and 872–880 K. CrB_4 and α-Fe phases were observed for the partially crystalline Gd1 alloy (Fig. 2(a)). In contrast, the peaks observed in the partially crystalline Gd5 alloy when heated to temperatures in the range of 872–880 K, correspond to the GdB_6, CrB_4, and FeB phases (Fig. 2(b)). The difference in the DSC scans of both Gd1 and Gd5 alloys (Fig. 1) can be attributed to the formation of dissimilar crystalline phases in the two alloys. Bright field (BF) TEM micrographs of partially crystalline alloys are presented in Fig. 3. They show a microstructure comprising of precipitates embedded in the amorphous matrix. As expected, the volume fraction of crystals within the amorphous matrix increases with higher annealing temperatures. For partially crystalline Gd1 alloys, the average size of the precipitates increases from 120 nm for annealing at 720 K to 147 nm at 740 K. For partially crystalline Gd5 alloys, average precipitate sizes of 27 nm at 872 K to 48 nm at 880 K were observed. This demonstrates precipitate growth and increasing crystalline mass fraction with higher annealing temperatures.

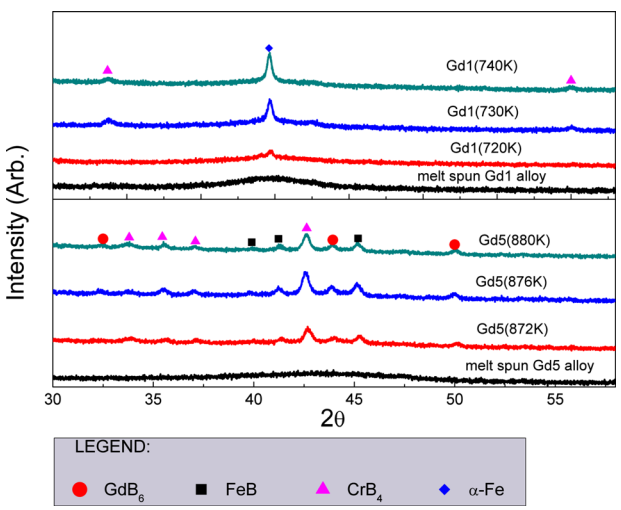

FIG. 2. XRD results of melt-spun and partially crystalline $Fe_{80-x}B_{12}Cr_8Gd_x$ alloys (x = 1 (a) and (b) 5 at. %, respectively).

The magnetic entropy change due to the application of a magnetic field (H) was calculated by the equation $\Delta S_M = \int_0^H (\partial M/\partial T)_H dH$, where the partial derivative is replaced by finite differences and numerical integration is performed. There are several definitions in the literature for RC, which measures the heat transfer between the hot and cold reservoirs.[23,24] In this work, RC is calculated in two ways: (a) RC_{FWHM}: the product of ΔS_M^{pk} times the full temperature width at half maximum of the peak (δT_{FWHM}) ($RC_{FWHM} = \Delta S_M^{pk} \cdot \delta T_{FWHM}$), and (b) RC_{AREA}: the numerical integration of the area under the $\Delta S_M(T)$ curves, using δT_{FWHM} as the integration limits.

The MCE of the partially crystalline alloys can only be investigated up to the crystallization temperatures of the amorphous matrix to avoid further microstructural evolution of the samples. Hence, the peak magnetic entropy change values ($|\Delta S_M^{pk}|$) were only observed near T_C of the residual amorphous matrix ($T_{C(am)}$).

The $\Delta S_M(T)$ curves (Fig. 4) show that annealing temperatures influenced differently the MCE behavior of partially crystalline Gd1 and Gd5 alloys. For Gd1 partially crystalline alloys, $|\Delta S_M^{pk}|$ decreased and T_C increased with increasing annealing temperatures. However, this trend was only observed for Gd5 (872 K) alloy when compared to its melt-spun counterpart (Fig. 4(b)). For Gd5 (876 K) and Gd5 (880 K) alloys, relatively constant $|\Delta S_M^{pk}|$ and T_C were observed. The different crystallization devitrification of Gd1 and Gd5 alloys influenced their MCE behavior.

The broad $|\Delta S_M^{pk}|$ values attained for partially crystalline Gd1 alloys annealed to higher annealing temperatures could be due to their broad ferromagnetic-paramagnetic phase transition, which has been reported for several multiphase MCM (such as Mo-containing Finemet,[5] Fe-B-Zr (Ref. 25), and Fe-B-Nb (Refs. 21, 22, and 26) based alloys), this phenomenon has also been observed in interacting superparamagnetic particles.[27,28] Their $|\Delta S_M^{pk}|$ values decreased because the $|\Delta S_M^{pk}|$ of their constituent phases were widely apart, consistent with the sum rule.[28] In addition, Jones *et al.* attributed the broadened $|\Delta S_M^{pk}|$ of Fe-Ni-Zr-B-Cu nanocomposite MCM to its asymmetric dependence of exchange interactions as well as the fluctuations of interatomic spacing within the amorphous matrix.[29]

The decrease of $|\Delta S_M^{pk}|$ for the Gd5 (872 K) alloy compared to that of the Gd5 melt-spun alloy is in agreement with

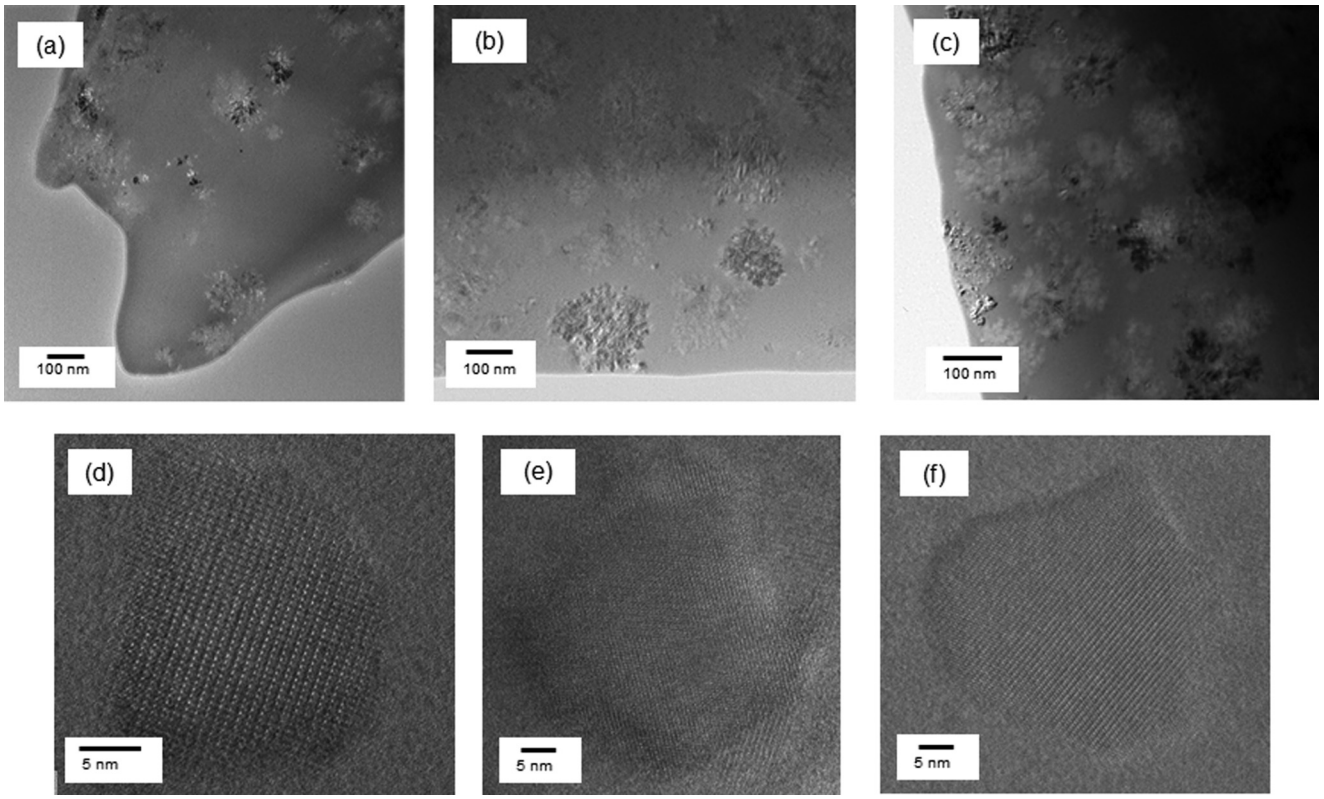

FIG. 3. BF TEM images of (a) Gd1(720 K), (b) Gd1(730 K), (c) Gd1(740 K), (d) Gd5(872 K), (e) Gd5(876 K), and (f) Gd5(880 K) alloys.

the sum rule.[28] The crystalline phases in partially crystalline Gd5 alloys are relatively less magnetic than the major crystalline α-Fe phase in partially crystalline Gd1 alloys, resulting in dissimilar MCE behavior, e.g., the relatively constant $|\Delta S_M^{pk}|$ observed in the Gd5 (876 K) and Gd5 (880 K) alloys. The increase in crystalline volume fraction in the partially crystalline alloys monotonically shifted the $T_{C(am)}$ to higher temperatures, this behavior is also observed in other Fe-based nanocrystalline MCM.[20,30–32] The increase in $T_{C(am)}$ with higher annealing temperatures has been attributed to the exchange field from the nanocrystalline precipitates penetrating into the residual amorphous matrix[20,30,32] and/or to the lowered Fe content in the amorphous matrix.[30] The compositional results obtained from EPMA measurements revealed good agreement with the nominal composition with oxygen content of ~0.71 wt. %. This oxygen content is the same in both amorphous and the partially crystalline samples, hence the change in T_C and $|\Delta S_M^{pk}|$ cannot be attributed to oxidation. Instead, the change in T_C and $|\Delta S_M^{pk}|$ is due to the formation, by partial crystallization, of the crystalline phase. This crystalline phase has a different composition from that of the amorphous matrix in which it is precipitated. Due to this change in the composition of the amorphous matrix the T_C and $|\Delta S_M^{pk}|$ are altered. This analysis is consistent with several previous papers, e.g., Refs. 20 and 30–33.

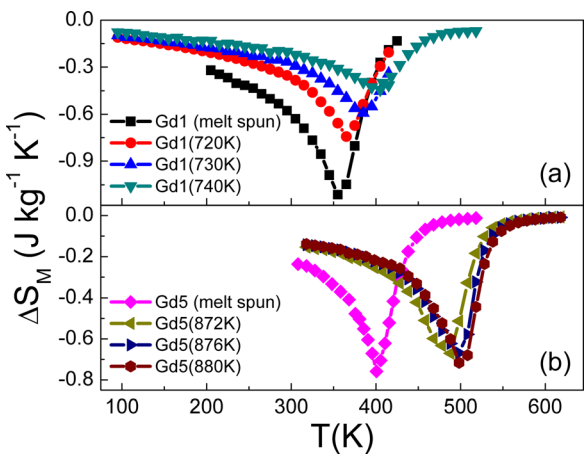

FIG. 4. Temperature dependence of the magnetic entropy change of partially crystalline (1.1 T) (a) Gd1 and (b) Gd5 alloys.

The properties of MCM are typically reported at the maximum available magnetic field in individual laboratories. Therefore, it is essential to study the magnetic field dependence of ΔS_M^{pk} and RC for comparison of different values reported in the literature. ΔS_M is dependent on the temperature and maximum applied field, the magnetic field dependence of ΔS_M can be expressed as a power law of the magnetic field:[34]

$$|\Delta S_M| \propto H^n. \tag{1}$$

At T_C, the exponent n becomes field independent and is expressed as

$$n(T_C) = 1 + \left(\frac{\beta - 1}{\beta + \gamma}\right), \tag{2}$$

where β and γ are the critical exponents.[34]

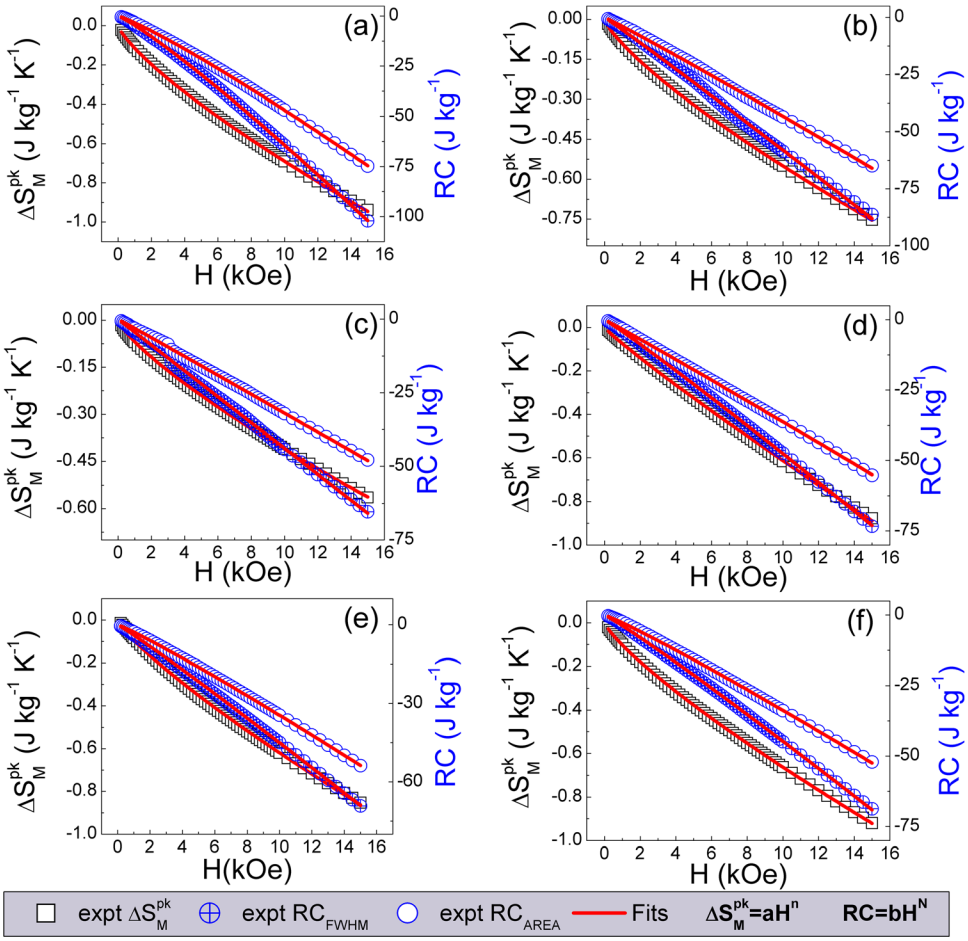

FIG. 5. Magnetic field dependence of (a) Gd1(720 K), (b) Gd1(730 K), (c) Gd1(740 K), Gd5(872 K), Gd5(876 K), and Gd5(880 K) alloys.

The scaling of RC with field is also controlled by the critical exponents of the MCM:[34]

$$RC_{FWHM} \propto H^{1+\frac{1}{\delta}}, \tag{3}$$

where the critical exponent δ can be determined from $\delta = 1 + \gamma/\beta$.[35]

The magnetic field dependence of ΔS_M^{pk} and RC of the partially crystalline Gd1 and Gd5 alloys are presented in Fig. 5. Good power law fit of the experimental $\Delta S_M^{pk}(H)$ and RC*(H)* data was observed. From the power law fit, the field dependence exponents governing $|\Delta S_M^{pk}|$ for these partially crystalline Gd1 and Gd5 alloys were determined to be 0.78 ± 0.01 and 0.85 ± 0.04, respectively. Consistent with theoretical predictions,[34] both $|RC_{FWHM}|$ and $|RC_{AREA}|$ scale with field using the same value of exponent $(1 + 1/\delta = 1.01 \pm 0.05$ and 1.08 ± 0.01 for partially crystalline Gd1 and Gd5 alloys, respectively). The $|\Delta S_M^{pk}|$ of partially crystalline Gd1 and Gd5 alloys compare favorably with those of Mo-containing Finemet-type nanocrystalline MCM;[5] T_C is lower. $|\Delta S_M^{pk}|$ of our partially crystalline Gd1 and Gd5 alloys are comparable to those of nanocrystalline Fe-Nb-B,[21] Fe-Nb-B-Cr,[22] Fe -Nb-B-Cr-Cu,[20] and Fe-Mo-Zr-Nb-B-Cu MCM.[9]

To enable the comparison of the perfomance of these materials with the literature data, the MCE characteristics of the partially crystalline alloys and the extrapolation of their MCE values to other magnetic fields are presented in Table I. It can be seen that as annealing temperatures increased, both $|\Delta S_M^{pk}|$ and RC decreased for partially crystalline Gd1,

TABLE I. Curie temperature and peak magnetic entropy change measured by VSM. Calculated field dependence of MCE extrapolated to magnetic fields of 5 T.

			$\lvert\Delta S_M^{pk}\rvert$ (J kg^{-1} K^{-1})		$\lvert RC_{FWHM}\rvert$ (J kg^{-1})		$\lvert RC_{AREA}\rvert$ (J kg^{-1})	
Nominal composition	T_C (K)	H (T)	1.5	5.0	1.5	5.0	1.5	5.0
Gd1 (720 K)	365		0.95	2.41	102	403	74	294
Gd1 (730 K)	385		0.75	1.92	89	310	66	231
Gd1 (740 K)	405		0.56	1.44	66	223	48	162
Gd5 (872 K)	488		0.89	2.68	56	200	54	193
Gd5 (876 K)	498		0.86	2.31	70	260	54	199
Gd5 (880 K)	498		0.92	2.45	70	260	53	195

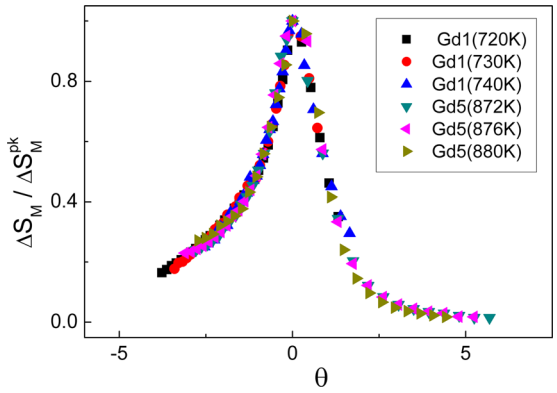

FIG. 6. Universal curve of Fe-B-Cr-Gd melt-spun and partially crystalline alloys.

and remained relatively constant for Gd5 partially crystalline alloys. Additionally, T_C increased with increasing annealing temperatures. These observations are in agreement with other previously reported for other partially crystalline Fe- and Gd-based alloy systems.[5,21,22,26,36]

The universal curves for MCE, which are constructed by a phenomenological procedure using experimental data, have been shown to be useful in rescaling $\Delta S_M(H,T)$ curves of different alloy compositions onto a single curve which is field-independent.[34,37,38] This procedure assumes that second order magnetic phase transition scales with field, i.e., all $M(H,T)$ curves should collapse onto a universal curve if they are appropriately presented,[34,37,38] leading to the collapse of $\Delta S_M(H,T)$ curves onto a single curve, since ΔS_M is obtained from magnetization data. Hence, the universal curve can be applied to characterize new MCM or as a technique to extrapolate magnetocaloric properties to magnetic fields and/or temperatures not easily accessible in the laboratories, enabling comparison of the performance of different MCM. Its construction is attained by (a) normalizing ΔS_M to its peak value (e.g., $\Delta S' = \Delta S_M(T)/\Delta S_M^{pk}$) and, (b) rescaling the temperature axis as:[34,37,38]

$$\theta = \begin{cases} -(T - T_C)/(T_{r_1} - T_c); & T_{r_1} < T_c \\ (T - T_C)/(T_{r_2} - T_c); & T_{r_2} > T_c, \end{cases} \quad (4)$$

where both T_{r_1} and T_{r_2} are reference temperatures such that $\Delta S_M(T_{r_i})/\Delta S_M^{pk} = 0.6$, $i = 1,2$.

Theoretical justifications for this procedure have been previously reported.[39] It is interesting to note that, using the phenomenological construction of the universal curve, all the normalized $\Delta S_M(T)$ curves of the partially crystalline alloys Gd1 and Gd5 alloys collapse onto a single curve (Fig. 6). This suggests that these alloys exhibit similar critical exponents, which agree with the observations from the field dependence exponents.

IV. CONCLUSIONS

The influence of annealing temperatures and crystallization on the MCE of $Fe_{80-x}B_{12}Cr_8Gd_x$ alloys (x = 1 and 5 at. %) was investigated by partially crystallizing their initial amorphous states. The different crystalline phases formed in these two alloys allow tuning of the RC and Curie temperature of the alloys.

- The MCE of the fully amorphous $Fe_{79}B_{12}Cr_8Gd_1$ and $Fe_{75}B_{12}Cr_8Gd_5$ alloys were found to be larger than those of their partially crystalline states. A decreasing trend of $|\Delta S_M^{pk}|$ with increasing annealing temperatures was observed for $Fe_{79}B_{12}Cr_8Gd_1$, similar to that of several multiphase Fe- and Gd-based MCM, while these magnitudes remain practically constant for $Fe_{75}B_{12}Cr_8Gd_5$.
- The Curie temperatures of the amorphous matrix of the partially crystalline $Fe_{79}B_{12}Cr_8Gd_1$ and $Fe_{75}B_{12}Cr_8Gd_5$ alloys were displaced to higher temperatures, similar to the behavior of several other nanocrystalline Fe-based MCM.
- The $|\Delta S_M^{pk}|$ of our partially crystalline $Fe_{79}B_{12}Cr_8Gd_1$ and $Fe_{75}B_{12}Cr_8Gd_5$ alloys compare favorably to Mo-containing Finemet-type, Fe-Nb-B, Fe(Cr)-Nb-B, Fe-Cr-Nb-B-Cu, and Fe-Mo-Zr-Nb-B-Cu MCM.
- The universal curve for $\Delta S_M(T)$ as well as the theoretical predictions of a power law magnetic field dependence of $|\Delta S_M^{pk}|$ and |RC| was found to be applicable to the partially crystalline $Fe_{79}B_{12}Cr_8Gd_1$ alloys as well as the $Fe_{75}B_{12}Cr_8Gd_5$ alloys despite differences in the crystallization behavior. Both these partially crystalline alloys exhibit second order magnetic phase transitions and similar critical exponents.
- The constant $|\Delta S_M^{pk}|$ and RC of partially crystalline $Fe_{75}B_{12}Cr_8Gd_5$ alloys with tunable T_C, suggest that these alloys are promising for multilayer active magnetic regenerator applications.

ACKNOWLEDGMENTS

This work was supported by the US AOARD (AOARD-08-4018, program manager, Dr. K. Caster), the Spanish Ministry of Science and Innovation and EU FEDER (Project MAT 2010-20537), the PAI of the Regional Government of Andalucía (Project FQM-6462) and the United States Office of Naval Research (Project N00014-11-1-0311). J.Y.L. would like to thank School of Materials Science and Engineering (NTU) for funding the research attachment in Sevilla University as well as Dr. Stevin Snellius Pramana for the EPMA measurements.

[1]K. A. Gschneidner, Jr. and V. K. Pecharsky, Annu. Rev. Mater. Sci. **30**, 387 (2000).
[2]B. G. Shen, J. R. Sun, F. X. Hu, H. W. Zhang, and Z. H. Cheng, Adv. Mater. **21**, 4545 (2009).
[3]O. Gutfleisch, M. A. Willard, E. Brück, C. H. Chen, S. G. Sankar, and J. P. Liu, Adv. Mater. **23**, 821 (2011).
[4]A. M. Tishin and Y. I. Spichkin, *The Magnetocaloric Effect and Its Applications* (Institute of Physics, Bristol, 2003).
[5]V. Franco, J. S. Blazquez, C. F. Conde, and A. Conde, Appl. Phys. Lett. **88**, 042505 (2006).
[6]F. Johnson and R. D. Shull, J. Appl. Phys. **99**, 08K909 (2006).
[7]R. Caballero-Flores, V. Franco, A. Conde, K. E. Knipling, and M. A. Willard, Appl. Phys. Lett. **96**, 182506 (2010).
[8]P. Gorria, J. L. Sánchez Llamazares, P. Álvarez, M. José Pérez, J. Sánchez Marcos, and J. A. Blanco, J. Phys. D: Appl. Phys. **41**, 192003 (2008).
[9]D. Wang, K. Peng, B. Gu, Z. Han, S. Tang, W. Qin, and Y. Du, J. Alloys Compd. **358**, 312 (2003).
[10]Q. Zhang, J. Du, Y. B. Li, N. K. Sun, W. B. Cui, D. Li, and Z. D. Zhang, J. Appl. Phys. **101**, 123911 (2007).

[11]M. A. Richard, A. M. Rowe, and R. Chahine, J. Appl. Phys. **95**, 2146 (2004).
[12]C. E. Reid, J. A. Barclay, J. L. Hall, and S. Sarangi, J. Alloys Compd. **207–208**, 366 (1994).
[13]R. Caballero-Flores, V. Franco, A. Conde, K. E. Knipling, and M. A. Willard, Appl. Phys. Lett. **98**, 102505 (2011).
[14]A. Rowe, A. Tura, J. Dikeos, and R. Chahine, in *Proceedings of the International Green Energy Conference* (Waterloo, Ontario, 2005), p. 84.
[15]J. Dikeos, Master's thesis, University of Victoria, 2006.
[16]J. Y. Law, R. V. Ramanujan, and V. Franco, J. Alloys Compd. **508**, 14 (2010).
[17]J. Y. Law, V. Franco, and R. V. Ramanujan, Appl. Phys. Lett. **98**, 192503 (2011).
[18]V. Franco, A. Conde, and L. F. Kiss, J. Appl. Phys. **104**, 033903 (2008).
[19]V. Provenzano, A. J. Shapiro, and R. D. Shull, Nature **429**, 853 (2004).
[20]J. Kovác, P. Švec, and I. Škorvánek, Rev. Adv. Mater. Sci. **18**, 533 (2008).
[21]I. Škorvánek and J. Kovác, Czech. J. Phys. **54**, D189 (2004).
[22]I. Škorvánek, J. Kovác, J. Marcin, P. Svec, and D. Janičkovič, Mater. Sci. Eng., A **449–451**, 460 (2007).
[23]K. A. Gschneidner, Jr., V. K. Pecharsky, A. O. Pecharsky, and C. B. Zimm, Mater. Sci. Forum **315–317**, 69 (1999).
[24]M. E. Wood and W. H. Potter, Cryogenics **25**, 667 (1985).
[25]Y. Wang and X. Bi, Appl. Phys. Lett. **95**, 262501 (2009).
[26]J. J. Ipus, J. S. Blazquez, V. Franco, A. Conde, and L. F. Kiss, J. Appl. Phys. **105**, 123922 (2009).
[27]L. H. Bennett, R. D. McMichael, L. J. Swartzendruber, R. D. Shull, and R. E. Watson, J. Magn. Magn. Mater. **104–107**, 1094 (1992).
[28]R. D. McMichael, R. D. Shull, L. J. Swartzendruber, L. H. Bennett, and R. E. Watson, J. Magn. Magn. Mater. **111**, 29 (1992).
[29]N. J. Jones, H. Ucar, J. J. Ipus, M. E. McHenry, and D. E. Laughlin, J. Appl. Phys. **111**, 07A334 (2012).
[30]I. Skorvánek, P. Svec, J.-M. Grenèche, J. Kovác, and J. M. Gerling, J. Phys.: Condens. Matter **14**, 4717 (2002).
[31]J. S. Garitaonandia, D. S. Schmool, and J. M. Barandiarán, Phys. Rev. B **58**, 12147 (1998).
[32]A. Hernando, I. Navarro, and P. Gorría, Phys. Rev. B **51**, 3281 (1995).
[33]R. Caballero-Flores, V. Franco, A. Conde, Q. Y. Dong, and H. W. Zhang, J. Magn. Magn. Mater. **322**, 804 (2010).
[34]V. Franco and A. Conde, Int. J. Refrig. **33**, 465 (2010).
[35]B. Widom, J. Chem. Phys. **43**, 3898 (1965).
[36]H. Fu, M. Zou, Q. Cao, V. K. Pecharsky, K. A. Gschneidner, Jr., and L. S. Chumbley, Mater. Sci. Eng., A **528**, 5219 (2011).
[37]V. Franco, A. Conde, J. M. Romero-Enrique, and J. S. Blázquez, J. Phys.: Condens. Matter **20**, 285207 (2008).
[38]V. Franco, J. S. Blázquez, and A. Conde, Appl. Phys. Lett. **89**, 222512 (2006).
[39]A. Arrott and J. E. Noakes, Phys. Rev. Lett. **19**, 786 (1967).